Journal of Photochemistry and Photobiology A: Chemistry 205 (2009) 122–128

Contents lists available at ScienceDirect

Journal of Photochemistry and Photobiology A: Chemistry

journal homepage: www.elsevier.com/locate/jphotochem

Novel leaf-shaped hybrid micro-particles: Chemically bonded self-assembly, microstructure and photoluminescence

Bing Yan*, Hai-Feng Lu

Department of Chemistry, Tongji University, Siping Road 1239, Shanghai 200092, PR China

ARTICLE INFO

Article history:
Received 29 November 2008
Received in revised form 10 April 2009
Accepted 22 April 2009
Available online 3 May 2009

Keywords:
Hybrid micro-particle
Chemically bonded
Microstructure
Photoluminescence

ABSTRACT

A series of hybrid micro-particles have been prepared from functionalized benzimidazole-5-carboxylic acid (BMZC) through an organization process under the coordination to RE^{3+} (Eu^{3+}, Tb^{3+}), whose leaf-shaped morphology and photoluminescence are studied. The coordination effect of rare earth ions has great influence on the sol–gel assembly reaction, the microstructure and luminescent behavior.

1. Introduction

Lanthanide complexes have been well known to give sharp and intense emissions under the irradiation of ultraviolet light [1]. The mechanism of those processes usually described as antenna effect: the ligand absorb the energy of ultraviolet light and transfer it to the lanthanide ion with high efficiency. Then the emission from the lanthanide ions' excited state will be observed [2]. Because of the excellence of lanthanide ion, lanthanide complexes are increasingly used in many devices, such as light-emitting diodes, luminescent probes, labels and sensors [3]. The major drawback of lanthanide complexes is their low thermal stabilities. So the lanthanide complexes are suitable only for applications in an appropriate temperature range. A way to solve these difficulties is to link these complexes to inorganic matrix with covalent bonds [4,5]. In these organic–inorganic matrices, usually designated as organically modified silicates, the multifunctional characters provided by the organic segments are combined with the thermal and mechanical stability of a siloxane-type network [4,5]. The development of novel linkages for tethering organic compounds to inorganic solid supports is an area of active investigation and there are five ways to synthesis lanthanide centered luminescent hybrid materials: amino-modification [6–8], hydroxyl-modification [9–11], carboxyl-modification [12–14], methylene-modification [15–17] and sulfide-modification [18,19].

Sol–gel method has been taken as the classical approach to prepare silica-based organic–inorganic hybrid materials due to the advantages such as low-temperature processing and easy shaping, higher sample homogeneity and purity [20]. Moreover, the location of the organic segments can be prior tuned through segments–matrix interactions (covalent bonds, hydrogen bonds, ionic and van der Waals bonds) [21]. Even when all the silica materials obtained by sol–gel route are always amorphous systems, the possibility of self-organization in these hybrid materials has been demonstrated by using very specific organic precursors such as linear spacers presenting rigid or semi-rigid geometries or a di-urea based precursor that exhibit a strong interaction by H-bonding [22–24]. In all the cases investigated, only weak interactions between the organic moieties such as van der Waals, London, or π–π staking were able to induce an organization. Thus, the introduction of an organic group appeared like a factor favorable for the existence of an organization into these amorphous systems since the X-ray scattering exhibits diffraction signals, but never any Bragg peak [25].

We use benzimidazole-5-carboxylic acid (BMZC) as the original reagent. It can react with 3-(triethoxysilyl)-propyl isocyanate. Then the precursor was submitted to complex with Eu^{3+}/Tb^{3+} ions and to a sol–gel process in order to obtain the anticipant hybrid materials. They are generally performed at room temperature where gelatine particles have to be stabilized by chemical cross-linking. As an alternative, we developed an oil-in-water (o/w) emulsion process involving the drying gelatine on a vacuum line, followed by the rapid condensation of silicates, leading to stable hybrid microparticles. The structure of the deposited silica particles appears to

* Corresponding author. Tel.: +86 21 65984663; fax: +86 21 65982287.
E-mail address: byan@tongji.edu.cn (B. Yan).

1010-6030/$ – see front matter © 2009 Elsevier B.V. All rights reserved.
doi:10.1016/j.jphotochem.2009.04.017

depend on both organosilane concentration and the coordination interactions.

2. Experimental

2.1. Chemicals and procedures

Starting materials were purchased from Aldrich or Fluka and were used as received. All normal organic solvents were purchased from China National Medicines Group and were distilled before utilization. Terbium and europium nitrates were obtained from the corresponding oxides in dilute nitric acid.

The synthesis of hybrid precursor BMZCSi (Fig. 1). The hybrid precursor was prepared as follows: 0.97 g (6 mmol) BMZC was first dissolved in 15 mL pyridine by stirring and then 1.48 g (6 mmol) 3-(triethoxysilyl)-propyl isocyanate was added to the solution by drops. The whole mixture was refluxing at 70 °C for 6 h. The solution was condensed to evaporate the solvent and then the residue was dried on a vacuum line. A purple oil was obtained. Elemental analysis for BMZCSi: $C_{18}H_{27}N_3SiO_6$. Calcd: C, 52.79; H, 6.65; N, 10.26%. Found: C, 52.41; H, 6.42; N, 9.97%. ^{1}H NMR ($CDC1_3$, 500 MHz) 0.62 (t, 2H, H_3), 1.22 (t, 9H, H_1) 1.60 (m, 2H, H_4), 3.16 (q, 2H, H_5), 3.83 (q, 6H, H_2), 4.14 (t, 1H, H_6), 7.90 (d, 1H, H_8), 7.91 (d, 1H, H_7), 8.08 (s, 1H, H_{10}), 8.29 (s, 1H, H_9), 12.79 (s, 1H, H_{11}).

The sol–gel preparation of BMZC–Si hybrids (Fig. 1). 0.6 mmol hybrid precursor and 1.2 mmol tetraethoxysilane (TEOS) were dissolved in 5 mL ethanol with stirring. The mixture was agitated magnetically to achieve a single phase in a covered Teflon beaker for four hours, and then 30 mL water was added under gentle magnetic stirring to form an initial o/w macro-emulsion for an hour. After that, it was dried on a vacuum line at 60 °C immediately. After aged until the onset of gelation which occurred, the gels were collected for the physical properties studies.

The sol–gel preparation of Tb(Eu)–BMZC–Si hybrids containing rare earth ions was prepared as follows (Fig. 1). 0.6 mmol precursor was dissolved in 5 mL ethanol with stirring. 0.2 mmol $RE(NO_3)_3{\cdot}6H_2O$ (RE = Tb, Eu) and 1.2 mmol tetraethoxysilane (TEOS) were added into the solution. The mixture was agitated magnetically to achieve a single phase in a covered Teflon beaker for four hours, and then 30 mL water was added under gentle magnetic stirring to form an initial o/w macro-emulsion for an hour. After that, it was dried on a vacuum line at 60 °C immediately. After aged until the onset of gelation which occurred, the gels were collected for the physical properties studies. All the samples of these hybrids are opaque solids but there is no complex going out from the hybrid materials for they are linked through the Si–O bonding network from the hydrolysis and copolycondensation process. To investigate the phase of lanthanide ion in hybrids, terbium nitrates mixed simply in BMZC–Si was prepared according to the percentage composition of Tb⊂BMZC–Si.

2.2. Measurements

Fourier transform infrared (FTIR) spectra were measured within the 4000–400 cm^{-1} region on an (Nicolet model 5SXC) infrared spectrophotometer with the KBr pellet technique. ^{1}H NMR (Proton Nuclear Magnetic Resonance) spectra were recorded in $CDCl_3$ on a BRUKER AVANCE-500 spectrometer with tetramethylsilane

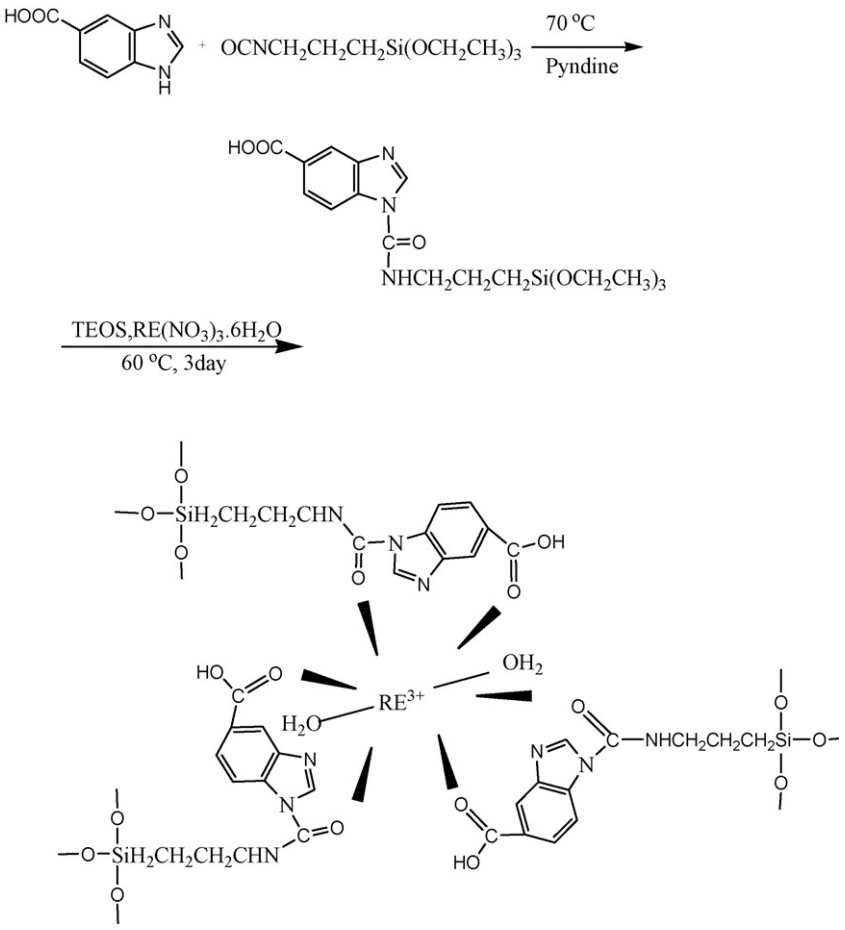

Fig. 1. Scheme for typical procedures for the preparation of BMZCSi and hybrid materials.

(TMS) as inter reference. Solid-state ^{29}Si magic-angle spinning (MAS) NMR spectrum was recorded at 79.46 MHz using a Bruker Avance 400 spectrometer. The chemical shifts were quoted in ppm from tetramethylsilane. Diffuse reflectance ultraviolet–visible spectra (DRUVS) of hybrid materials were recorded with a BWSpec 3.24u_42 spectrophotometer. Luminescence (excitation and emission) spectra of these solid complexes were determined with a RF-5301 spectrophotometer whose excitation and emission slits were 5 and 3 nm, respectively. And the fluorescence decay properties were recorded on an Edinburgh Analytical Instruments. The X-ray diffraction (XRD) measurements were carried out on powdered samples via a "BRUKER D8" diffractometer (40 mA_40 kV) using monochromated Cu $K_{\alpha 1}$ radiation (λ = 1.54 Å) over the 2θ range of 10–70°. Scanning electronic microscope (SEM) images were obtained with a Philps XL-30. The quantum yield of the samples was determined using an integrating sphere (150 mm diameter, $BaSO_4$ coating) of Edinburgh Instruments. The quantum yield can be defined as the integrated intensity of the luminescence signal divided by the integrated intensity of the absorption signal. Only the intense luminescence band of the $^5D_0 \rightarrow {}^7F_2$ transition around 612 nm was measured by the integrating sphere, but this intensity value was corrected by taking into account the relative intensity of the other transitions (as determined from the steady-state luminescence spectrum in the 550–750 nm region). In this way, an intensity value that corresponds to the total luminescence output was obtained. The absorption intensity was calculated by subtracting the integrated intensity of the light source with the sample in the integrating sphere, from the integrated intensity of the light source with a blank sample in the integrating sphere. Two similar cuvettes were used for both the solid sample (which was placed inside the cuvette) and the reference solution. Care was taken to obtain a reproducible placement of the cuvette in the integration sphere.

3. Results and discussion

The Fourier Transform Infrared spectra (FTIR) for BMZC (a), the precursor BMZCSi (b), BMZC–Si hybrids (c) and Tb–BMZC–Si hybrids (d) are shown in Fig. 2.Three adjacent sharp peaks at 2982 cm^{-1}, 2934 cm^{-1} and 2886 cm^{-1} in curve of precursors (b) are $\nu_{as}(CH_2)$ and $\nu_s(CH_2)$ of the long carbon chain in precursors. And ^{1}H NMR spectra relative to the precursors are in full agreement with the proposed structures. In the spectra of hybrid materials, the spectra are dominated by the ν(Si–O–Si) absorption bands at 1120–1000 cm^{-1}. These indicated the formation of siloxane bonds. The ν(O–H) came from the absorbed water in the hybrid material. The ν(Si–C) vibration located in the 1173 cm^{-1} in IR spectra of hybrid materials was consistent with the fact that no (Si–C) bond cleavage occurred during modification, hydrolysis and condensation reactions. The decrease of other peaks' intensities may be due to the containing of the organic groups by the silicate inorganic host which occurred in the hydrolysis and condensation process. Coordination of lanthanide ions by the ligands is clearly shown by infrared spectroscopy. In spectrum of precursors (b), the $\nu(COO^-)_{as}$ vibrations is located at 1730 cm^{-1} and the $\nu(COO^-)_{sy}$ vibrations is located at 1417 cm^{-1}. But in the spectrum of the hybrid material II (d), the $\nu(COO^-)_{sy}$ vibration is shifted to the 1384 cm^{-1} while it is still located at 1417 cm^{-1} in the BMZC–Si (c). The shift is a proof of the coordination of the carboxylic group to the metallic ion with the oxygen atoms.

Furtherly, the selected ^{29}Si MAS NMR spectrum of Tb–BMZC–Si hybrids is displayed in Fig. 3. Distinct resonances can be observed

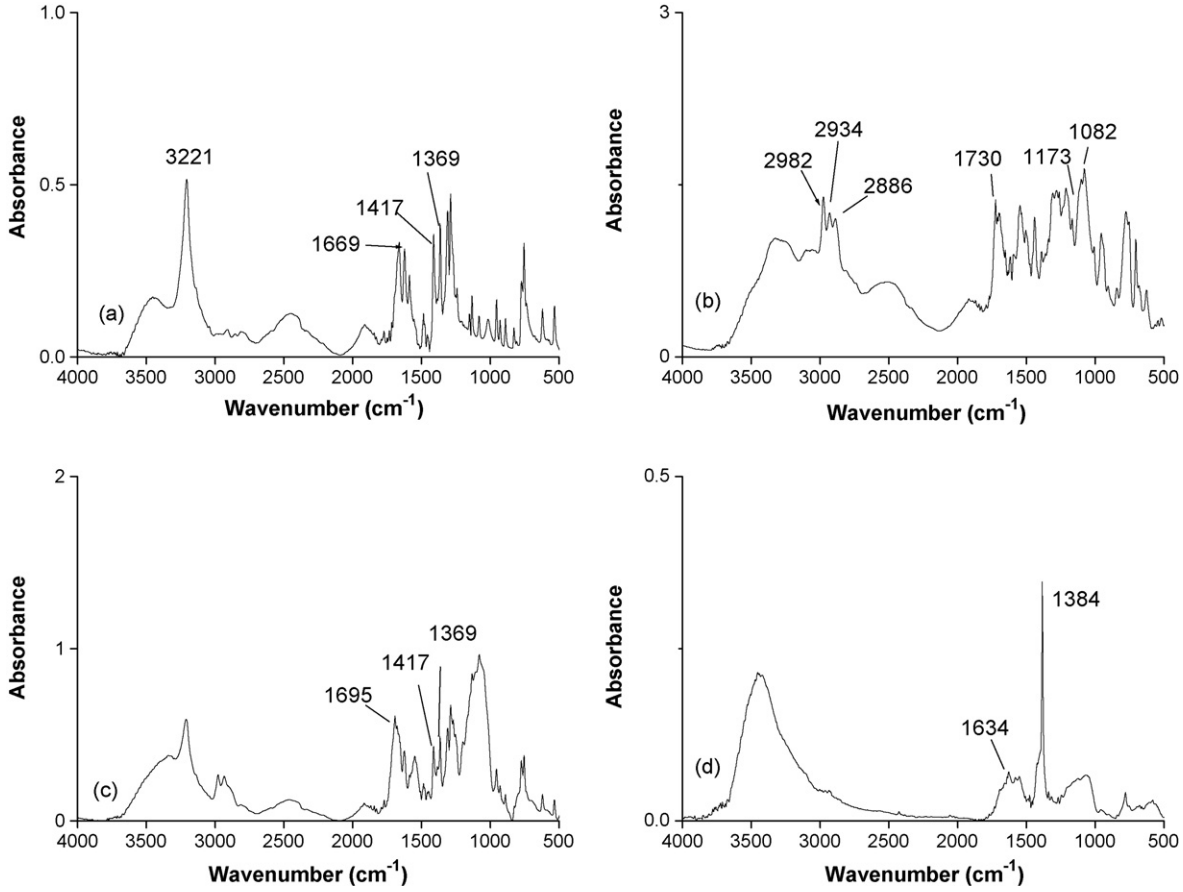

Fig. 2. Infrared spectra for BMZC (a), the precursor BMZCSi (b), hybrid material BMZC–Si (c) and Tb–BMZC–Si (d).

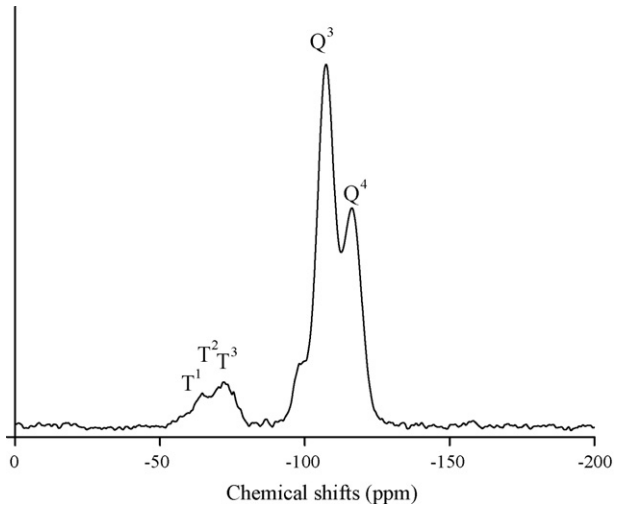

Fig. 3. Selected ^{29}Si MAS NMR spectrum of Tb–BMZC–Si hybrids.

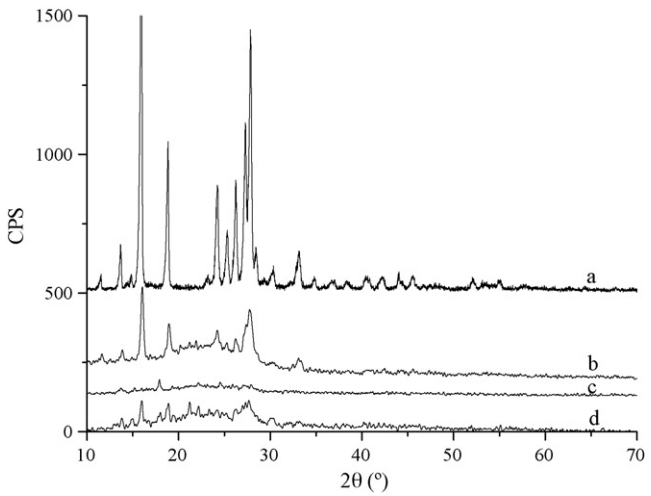

Fig. 5. The X-ray diffraction graphs of BMZC (a), BMZCSi (b), Tb–BMZC–Si hybrid material (c) and Tb⊂BMZC–Si (d).

for the siloxane [Q^n = Si–$(OSi)_n(OH)_{4-n}$, n = 2–4] and organosiloxane [T^m = R–Si–$(OSi)_m(OH)_{3-m}$, m = 1–3] species [26–28]. The relative integrated intensities of the organosiloxane T^1, T^2, and T^3 NMR signals can be employed to estimate the degree of hydrolysis-condensation of organic functional groups [26–28]. Compared with T^1 and T^2 organosiloxane centers, the predominance of T^3 [the T^3:(T^3 + T^2 + T^1) ratio is 0.73] and no T^0 peaks suggest that the hydrolysis and condensation reactions of the organic functionality (BMZC–Si) in the ordered structure are nearly complete, indicating a strong linkage (three Si–O–Si covalent bonds) between the organic ligand and the silica matrix [26–28].

The phosphorescence spectrum of the precursor is recorded (Fig. 4). The curve exhibited a broad phosphorescence band which corresponds to the triplet state emission of the precursor. The peak is located at 430 nm. So the triplet state energy of precursor is 23,255 cm^{-1} in the precursor. According to the energy transfer and intra-molecular energy mechanism [29,30], it can be predicted that the triplet state energy of precursor is more suitable for the luminescence of terbium ion (20,500 cm^{-1}) than europium ion (17,250 cm^{-1}). When the gap of the energy levels between the ligand and europium ion is large, the energy transfer will be hampered.

The X-ray diffraction graphs of BMZC, BMZC–Si hybrids, Tb–BMZC–Si hybrids and Tb⊂BMZC–Si hybrids are shown in Fig. 5.

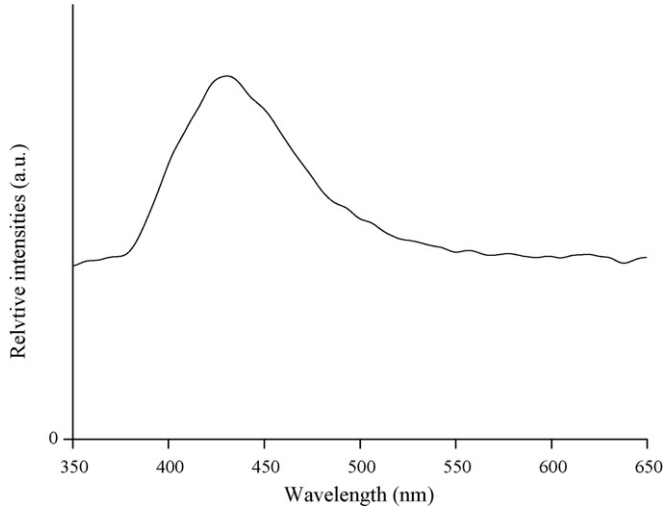

Fig. 4. The phosphorescence spectrum of BMZCSi.

In the spectrum of BMZC, there are characteristic X-radiation peaks of BMZC crystals. However, the diffractogram of hybrid materials reveals that all of the hybrid materials with $10^\circ \le n \le 70^\circ$ are mostly amorphous. To BMZC–Si hybrids, there are several small peaks protruding from the baseline which are attributed to the regular arrangement of the organic groups. What is more, there are totally amorphous in the Tb–BMZC–Si hybrids. To exclude the impact of lanthanide nitrates, the XRD spectrum of Tb⊂BMZC–Si hybrids is measured. Between BMZC–Si hybrids and Tb⊂BMZC–Si hybrids, some peaks protrude around 22° and the intensities of narrow peaks decrease which means that the peaks of terbium nitrate is located around 22° and simply mix could not lead to a total amorphous. Comparing Tb–BMZC–Si with Tb⊂BMZC–Si, the peaks of terbium nitrates and the peaks appeared in BMZC–Si are all disappeared which means that the lanthanide ions coordinated with ligand in the host other than terbium nitrates. It can be concluded that because of the coordination between lanthanide ions and the precursors the regular arrangement of the organic groups in BMZC–Si are disturbed.

The scanning electron micrographs (SEM) of these hybrid materials can give some proofs from the texture. Fig. 6 demonstrates that micro-particle materials were obtained. In the sol process, the o/w macro-emulsion is decisive and responsible for the materials' final texture. The texture of lamina is easy to understand because the weak interactions between the organic moieties such as van der Waals, London, or π–π staking were able to induce an organization in o/w macro-emulsion [22–24]. These images for the hybrid materials demonstrate that a homogeneous, molecular-based material was obtained where no phase separation was observed because of strong covalent bonds bridging between the inorganic and organic phases. In addition, uniform leaf-shaped micro-particles can be observed on the surface of the hybrid material, mainly through the formation of the backbone of Si–O–Si and its polycondensation. The micro-particle BMZC–Si is located in around 0.5–1 μm dimension. The texture of Tb–BMZC–Si and Eu–BMZC–Si seem to be slightly different with BMZC–Si because they were prepared by same process. But the texture of agglomerate in BMZC–Si disappeared in Tb(Eu)–BMZC–Si. And the texture of Tb(Eu)–BMZC–Si is more uniform. It may be owing to the coordination between organic groups and lanthanide ions that the configurations of the organosilane are mixed up and it is difficult to form a large organization, whose particle sizes are in the 0.1–0.2 μm dimension. Because of the different chelation effect between organic groups and Tb^{3+} or Eu^{3+} ions, the configurations of the organosilane is mixed up and it is difficult to

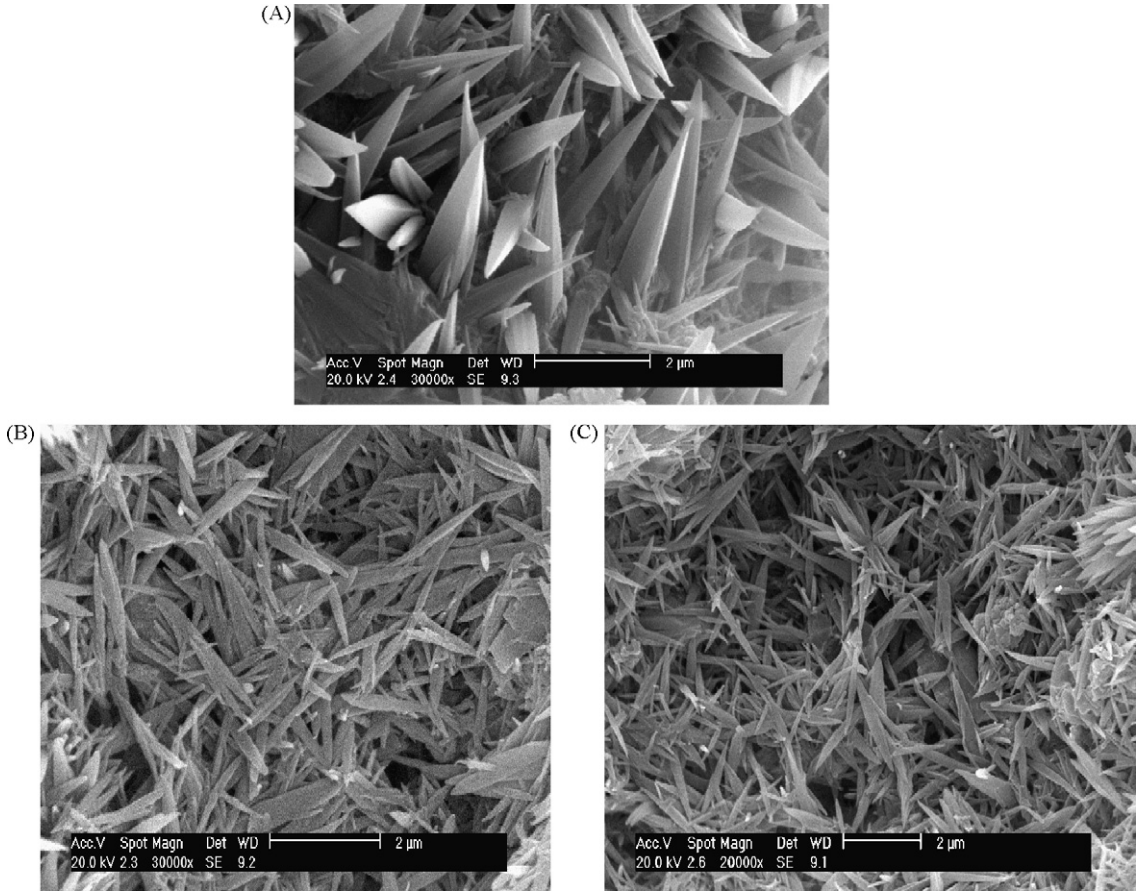

Fig. 6. The scanning electron micrographs of the covalently bonded hybrid micro-particles: BMZC–Si (A), Eu–BMZC–Si (B) and Tb–BMZC–Si (C).

form an organization under the weak interactions such as π–π staking. As mentioned in the experimental, the hybrid materials could be received through a polycondensation reaction between the terminal silanol groups of BMZCSi and the OH groups of hydrolyzed TEOS. At the beginning of the reaction, the individual hydrolysis of BMZCSi and TEOS are predominant. The next step is related to the polycondensation reactions between hydroxyl groups of both BMZCSi and TEOS. By these methods, the covalently bonded hybrids BMZC–Si can be achieved. Similarly, the molecular-based composites bearing the RE–O coordination bond and Si–O covalent bonds can also been obtained after the introduction of Tb^{3+} or Eu^{3+}. It is worthy pointing out that the self-assembly phenomenon exists in the non-crystalline hybrid systems through chemical bonding (covalent bonding and coordination bonding, strong interaction), which is hardly to be reported.

The diffuse reflectance ultraviolet-visible spectra (DRUVS) of BMZC, BMZC–Si and Tb–BMZC–Si are shown in Fig. 7(a). In the spectra, the absorption peak around 300 nm corresponded to the $\pi \rightarrow \pi^*$ electronic transition of carboxylic acid group. The similarities among three kinds of materials prove that the modification of the BMZC–Si did not change the energy level of the carboxylic acid group. Fig. 7(b) is the excitation spectra of the resulting hybrid materials, which is monitored at 545 nm under room temperature. The spectra exhibits a broad excitation bands centered at 300 nm in the UV range. The excitation spectrum is consistent with the ultraviolet spectra.

The luminescence behaviors of all of the materials have been investigated at 298 K by direct excitation of the ligand (300 nm). Fig. 8(A) illustrates typical photoluminescence spectra of the BMZC–Si. Because no lanthanide ions are doped in them, this kind of hybrid materials can only emit the luminescence of the whole organically modified Si–O network hybrid system (composed by organic group and Si–O matrix). There is a broad band from 420 to 550 nm (λ_{max} = 470 nm). Fig. 8(B) exhibits typical photoluminescence spectra of the Eu–BMZC–Si. The maxima of these bands are at 590 and 613 nm which is associated with $^5D_0 \rightarrow {}^7F_1$ and $^5D_0 \rightarrow {}^7F_2$ transitions, respectively. The energy transfer from the carboxylic ligand to europium (III) is not perfect, as can be noticed that the residual ligand emission before 550 nm is still strong. A prominent feature that may be noted in these spectra is the low intensity ratios of $I(^5D_0 \rightarrow {}^7F_2)/I(^5D_0 \rightarrow {}^7F_1)$. The intensity (the integration of the luminescent band) ratio of the $^5D_0 \rightarrow {}^7F_2$ transition to $^5D_0 \rightarrow {}^7F_1$ transition has been widely used as an indicator of Eu^{3+} site symmetry [31]. When the interactions of the rare-earth complex with its local chemical environment are stronger, the complex becomes more non-symmetrical and the intensity of the electric-dipolar transitions becomes more intense. As a result, $^5D_0 \rightarrow {}^7F_1$ transition (magnetic-dipolar transitions) decreased and $^5D_0 \rightarrow {}^7F_2$ transition (electric-dipolar transitions) increased. In this situation, the intensity ratios are approximately 2.3 which mean that the matrix did not disturb the coordination between the organic groups and lanthanide ions. Fig. 8(C) illustrates typical photoluminescence spectra of Tb–BMZC–Si hybrids. Narrow-width emission bands with maxima at 487 and 543 nm are recorded. These bands are related to the transition from the triplet state energy level of Tb^{3+} to the different single state levels and are attributed to the $^5D_4 \rightarrow {}^7F_6$ and $^5D_4 \rightarrow {}^7F_5$ transitions of Tb^{3+} ions. The lower baseline in the spectra suggests that energy transfer efficiency between the organic groups and Tb^{3+} ions is higher than that between the organic groups and Eu^{3+} ions.

The luminescence decays of the hybrid material fit a single-exponential rule ($\text{Fit} = A + B_1 \times \exp(-t/T_1)$), confirming that all

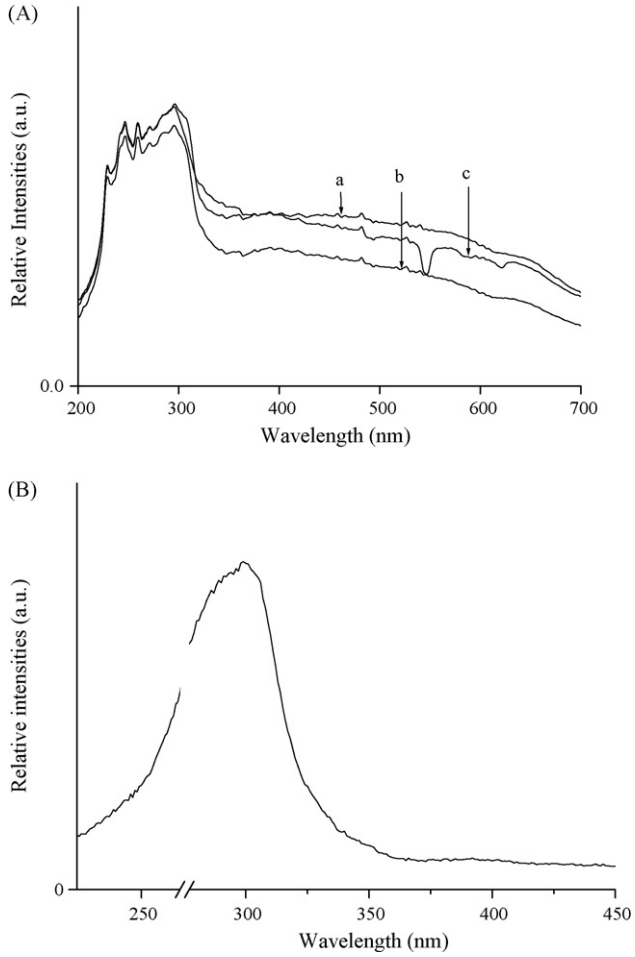

Fig. 7. (A) Diffuse reflectance ultraviolet–visible spectra (DRUVS) of BMZC (a), hybrid material BMZC–Si (b) and hybrid material Tb–BMZC–Si (c); (B) the excitation spectrum of BMZC–Si.

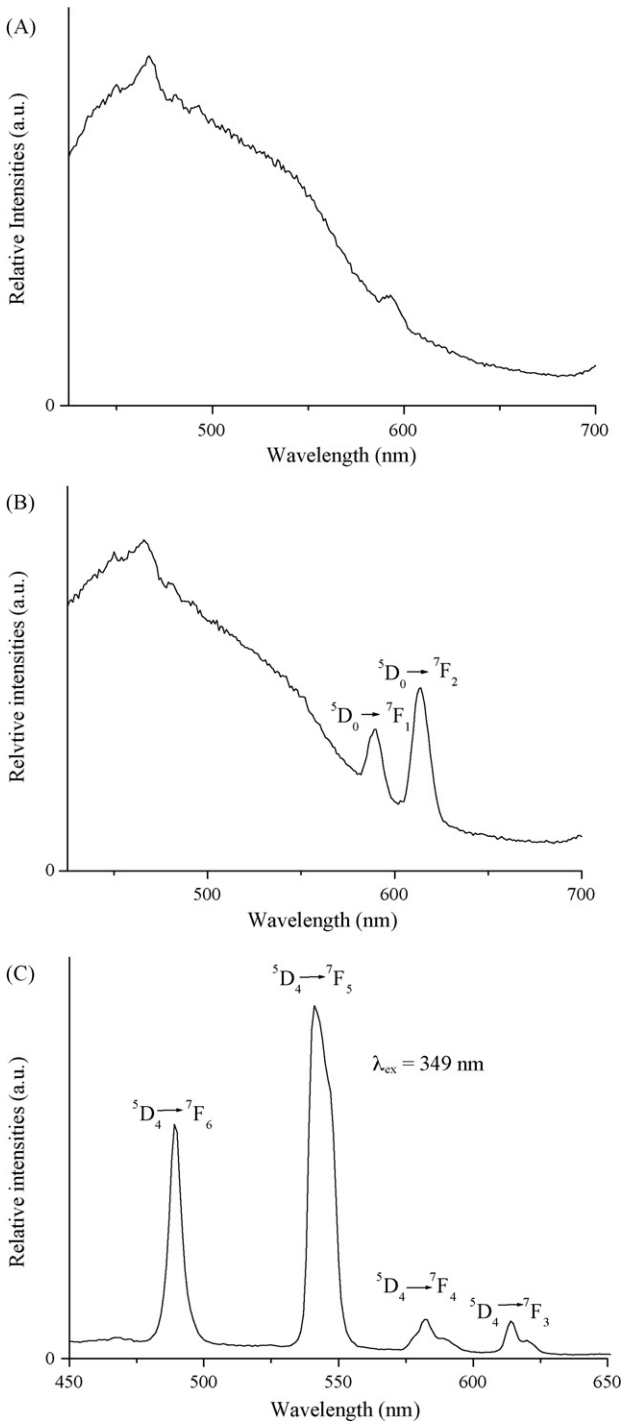

Fig. 8. Photoluminescence spectra of the covalently bonded hybrid micro-particles: BMZC–Si (A), Eu–BMZC–Si (B) and Tb–BMZC–Si (C).

lanthanide ions lie in the same coordination environment. The resulting lifetime of the europium and terbium hybrids is 0.615 and 0.965 ms, respectively. What is more, it appears as a general trend that the lifetimes in this hybrid material are similar as those in the corresponding organic complexes which range is from 0.2 to 1.7 ms, indicating an important maintenance of luminescent stability for the covalently bonded molecular network in the hybrid systems. The luminescent lifetime of terbium hybrids is longer than that of europium ones, which is the similar order to the luminescent intensity, indicating both BMZC–Si show the more suitable for the luminescence of Tb^{3+} than Eu^{3+}. The quantum yield of them was determined using an integrating sphere (150 mm diameter, $BaSO_4$ coating) of Edinburgh Instruments. The spectra were corrected. The quantum yield can be defined as the integrated intensity of the luminescence signal divided by the integrated intensity of the absorption signal. Only the intense luminescence band of the $^5D_0 \rightarrow {}^7F_2$ transition around 612 nm was measured by the integrating sphere, but this intensity value was corrected by taking into account the relative intensity of the other transitions (as determined from the steady-state luminescence spectrum in the 550–750 nm region). In this way, an intensity value that corresponds to the total luminescence output was obtained. Comparing the value of luminescent quantum efficiencies, it can be found that they show the similar rule to the value of luminescent lifetimes. The luminescent quantum efficiency of terbium hybrids (24.5%) is higher than that of europium one (7.7%), suggesting the fact of different energy match and intra-molecular energy transfer process. At last, we can predict the energy transfer efficiencies for the two covalently bonded lanthanide hybrid materials [32,33]. For Eu–BMZC–Si and Tb–BMZC–Si, BMZC–Si can be considered as the host and the energy donor for Eu^{3+} or Tb^{3+} (energy acceptor) with luminescent quantum efficiency of 29.4%. On the basis of the references [32,33], the energy transfer efficiency from BMZC–Si to Eu^{3+} in Eu–BMZC–Si hybrids (26%) is much lower than that between BMZC–Si and Tb^{3+} in Tb–BMZC–Si hybrids (83%). The higher energy transfer efficiency for Tb hybrids leads to the higher luminescent quantum efficiency.

4. Conclusions

A novel kind of aromatic carboxylic acid, benzimidazole-5-carboxylic acid (abbreviated as BMZC) is modified by 3-(triethoxysilyl)-propyl isocyanate through the hydrogen atom transfer addition reaction. Then the functionalized molecular precursor (BMZCSi) occurs a sol–gel assembly process under the induced coordination effect of RE^{3+} (Eu^{3+}, Tb^{3+}), resulting in a series of chemically bonded hybrid micro-particles. The microstructure and photoluminescence have been studied in details. Especially the hybrids present interesting leaf-shaped morphology. The coordination effect of rare earth ions has great influence on the sol–gel assembly reaction, the microstructure and luminescent behavior.

Acknowledgements

This work was supported by the National Natural Science Foundation of China (20671072) and Program for New Century Excellent Talents in University (NCET-08-0398).

References

[1] L.R. Matthews, E.T. Knobbe, Luminescence behavior of europium complexes in sol–gel derived host materials, Chem. Mater. 5 (1993) 1697–1700.
[2] G. Crosby, R.E. Whan, R. Alire, Intramolecular energy transfer in rare earth chelates: role of the triplet state, J. Chem. Phys. 34 (1961) 743–748.
[3] G. Blass, B.C. Grabmaier, Luminescent Materials, Springer, Berlin, 1994.
[4] C. Sanchez, F. Ribot, Design of hybrid organic–inorganic materials synthesized via sol–gel chemistry, New J. Chem. 18 (1994) 1007–1047.
[5] M.C. Goncalves, N.J.O. Silva, V.D.Z. Bermudez, R.A.S. Ferreira, L.D. Carlos, K. Dahmouche, C.V. Santilli, D. Ostrovskii, I.C.C. Vilela, A.F. Craievich, Local structure and near-infrared emission features of neodymium-based amine functionalized organic/inorganic hybrids, J. Phys. Chem. B 109 (2005) 20093–20104.
[6] H.R. Li, J. Lin, H.J. Zhang, L.S. Fu, Q.G. Meng, S.B. Wang, Preparation and luminescence properties of hybrid materials containing europium (III) complexes covalently bonded to a silica matrix, Chem. Mater. 14 (2002) 3651–3655.
[7] Q.M. Wang, B. Yan, Novel luminescent terbium molecular-based hybrids with modified meta aminobenzoic acid covalently bonded with silica, J. Mater. Chem. 14 (2004) 2450–2455.
[8] Q.M. Wang, B. Yan, Assembly of red and green nanophosphors from amine-functionalized covalent linking hybrids with emitting centers Eu^{3+} and Tb^{3+} ions, J. Photochem. Photobiol. A Chem. 178 (2006) 70–75.
[9] A.C. Franville, D. Zambon, R. Mahiou, Y. Troin, Luminescence behavior of sol–gel-derived hybrid materials resulting from covalent grafting of a chromophore unit to different organically modified alkoxysilanes, Chem. Mater. 12 (2000) 428–435.
[10] Q.M. Wang, B. Yan, A novel way to luminescent terbium molecular-scale hybrid materials: modified heterocyclic ligands covalently bonded with silica, Cryst. Growth Des. 5 (2005) 497–503.
[11] Q.M. Wang, B. Yan, Construction of lanthanide luminescent molecular-based hybrid material using modified functional bridge chemically bonded with silica, J. Photochem. Photobiol. A Chem. 175 (2006) 159–165.
[12] Y.L. Sui, B. Yan, Fabrication and photoluminescence of molecular hybrid films based on the complexes of 8-hydroxyquinoline with different metal ions via sol–gel process, J. Photochem. Photobiol. A Chem. 182 (2006) 1–6.
[13] B. Yan, X.F. Qiao, Photophysical properties of terbium molecular hybrids assembled with novel ureasil linkages, Photochem. Photobiol. 83 (2007) 971–978.
[14] J.L. Liu, B. Yan, Molecular construction and photophysical properties of luminescent covalently bonded lanthanide hybrid materials obtained by grafting organic ligands containing 1,2,4-triazole on silica by mercapto modification, J. Phys. Chem. C 112 (2008) 14168–14178.
[15] B. Yan, B. Zhou, Two photoactive lanthanide (Eu^{3+} Tb^{3+}) hybrid materials by modified β-diketone bridge directly covalently bonded mesoporous host (MCM-41), J. Photochem. Photobiol. A Chem. 195 (2008) 314–322.
[16] Y. Li, B. Yan, H. Yang, Construction, characterization and photoluminescence of mesoporous hybrids containing europium (III) complexes covalently bonded to SBA-15 directly functionalized by modified β-diketone, J. Phys. Chem. C 112 (2008) 3959–3968.
[17] B. Yan, Q.M. Wang, First two luminescent molecular hybrids composed of bridged Eu(III)–β-diketone chelates covalently trapped in silica and titanate gels, Cryst. Growth Des. 6 (2008) 1484–1489.
[18] B. Yan, H.F. Lu, Lanthanide centered covalently bonded hybrids through sulfide linkage: molecular assembly, physical characterization and photoluminescence, Inorg. Chem. 47 (2008) 5601–5611.
[19] J.L. Liu, B. Yan, Lanthanide, (Eu^{3+}, Tb^{3+}) centered hybrid materials using modified functional bridge chemical bonded with silica: molecular design, physical characterization, and photophysical properties, J. Phys. Chem. B 112 (2008) 10898–10907.
[20] U. Schubert, N. Husing, A. Lorenz, Hybrid inorganic–organic materials by sol–gel processing of organofunctional metal alkoxides, Chem. Mater. 7 (1995) 2010–2027.
[21] C. Sanchez, B. Lebeau, F. Chaput, J.P. Boilot, Optical properties of functional hybrid organic–inorganic nanocomposites, Adv. Mater. 15 (2003) 1969–1994.
[22] S. Inagaki, S. Guan, T. Ohsuna, O. Terasaki, An ordered mesoporous organosilica hybrid material with a crystal-like wall structure, Nature 416 (2002) 304–307.
[23] J.J.E. Moreau, L. Vellutim, M.W.C. Man, C. Bied, New hybrid organic–inorganic solids with helical morphology via H-bond mediated sol–gel hydrolysis of silyl derivatives of chiral (R,R)- or (S,S)-diureidocyclohexane, J. Am. Chem. Soc. 123 (2001) 1509–1510.
[24] J.J.E. Moreau, L. Vellutim, M.W.C. Man, C. Bied, J.L. Bantignles, P. Dieudonne, J.L. Sauvajol, Self-organized hybrid silica with long-range ordered lamellar structure, J. Am. Chem. Soc. 123 (2001) 7957–7958.
[25] G. Cerveau, R.J.P. Corriu, E. Framery, F. Lerouge, Auto-organization of nanostructured organic–inorganic hybrid xerogels prepared by sol–gel processing: the case of a "twisted" allenic precursor, Chem. Mater. 16 (2004) 3794–3799.
[26] M.C. Gonalves, V.D.Z. Bermudez, R.A.S. Ferreira, L.D. Carlos, D. Ostrovskii, J. Rocha, Optically functional di-urethanesil nanohybrids containing Eu^{3+} ions, Chem. Mater. 16 (2004) 2530–2543.
[27] W.S. Kim, M.G. Kim, J.H. Ahn, B.S. Bae, C.B. Park, Protein micropatterning on bifunctional organic–inorganic sol–gel hybrid materials, Langmuir 23 (2007) 4732–4736.
[28] C.Y. Peng, H.J. Zhang, J.B. Yu, Q.G. Meng, L.S. Fu, H.R. Li, L.N. Sun, X.M. Guo, Synthesis, characterization, and luminescence properties of the ternary europium complex covalently bonded to mesoporous SBA-15, J. Phys. Chem. B 109 (2005) 15278–15287.
[29] S. Sato, W. Mada, Relations between intramolecular energy transfer efficiencies and triplet state energies in rare earth β-diketone chelates, Bull. Chem. Soc. 43 (1970) 1955–1966.
[30] Q.M. Wang, B. Yan, X.H. Zhang, Photophysical properties of novel lanthanide complexes with long chain mono-eicosyl *cis*-butene dicarboxylate, J. Photochem. Photobiol. A Chem. 174 (2005) 119–124.
[31] Z. Wang, J. Wang, H.J. Zhang, Luminescent sol–gel thin films based on europium-substituted heteropolytungstates, Mater. Chem. Phys. 87 (2004) 44–48.
[32] P.R. Biju, G. Jose, V. Thomas, V.P.N. Nampoori, N.V. Unnikrishnan, Energy transfer in Sm^{3+}:Eu^{3+} system in zinc sodium phosphate glasses, Opt. Mater. 24 (2004) 671–677.
[33] P.P. Lima, S.S. Nobre, R.O. Freire, S.A. Junior, L. Mafra, R.A.S. Ferreira, U. Pischel, O.L. Malta, L.D. Carlos, Energy transfer mechanisms in organic–inorganic hybrids incorporating europium(III): a quantitative assessment by light emission spectroscopy, J. Phys. Chem. C 111 (2007) 17627–17634.